Supporting Information

Emerging Lead-Free All Inorganic Perovskite Single Crystals $K_7Bi_3X_{16}$ (X=Cl, Br) toward Photodetector Application

Wenjian Yang [#a], Jingshen Zhang[# a], Hui Xiong [a], Jing Lan [a], Songyang Yuan[a], Mengdi Zhan [a], Ziyu Tan [a], Wenzhe Li* [b,c,d], Jiandong Fan* [b,c,d]

[a] Department of Electronic Engineering, College of Information Science and Technology, Jinan University, Guangzhou, 510632, China

[b] Institute of New Energy Technology, College of Physics & Optoelectronic Engineering, Jinan University, Guangzhou, 510632, Guangdong, China

[c] Key Laboratory of New Semiconductors and Devices of Guangdong Higher Education Institutes, Jinan University, Guangzhou, 510631, China

[d] Guangdong Provincial Key Laboratory of Nanophotonic Manipulation, Jinan University, Guangzhou 511443, China. li_wz16@jnu.edu.cn, jdfan@jnu.edu.cn

[#] The authors contributed equally to this work

Content

$K_7Bi_3X_{16}$(X=Cl, Br) perovskite single crystal growth. The $K_7Bi_3Cl_{16}$ and $K_7Bi_3Br_{16}$ perovskite single crystals were hydrothermally prepared by the method of temperature cooling crystallization. For the $K_7Bi_3Cl_{16}$ perovskite single crystal, 0.2714g potassium chloride (KCl, Aladdin, 99.99%) and 1.5767g bismuth chloride ($BiCl_3$, Macklin, 99.99%) were mixed with 2.4 ml hydrochloric acid (HCl, Guangzhou Chemical Reagent Factory, 31%). For the $K_7Bi_3Br_{16}$ perovskite single crystals, 0.1251g potassium bromide (KBr, Aladdin, 99%) and 1.0302g bismuth bromide ($BiBr_3$, Macklin, 98%) were mixed with 1 ml hydrobromic acid (HBr, Aladdin, 48 wt. % in H_2O, 99.99%). The method they both applied was identical. The solution was heated on the hotplate under the temperature of 140℃ for 1h for complete dissolution. Then the temperature decreased by the rate of 1.5℃/h from 140℃ to 30℃. Finally, at the bottom of glass bottle six-sided crystals of $K_7Bi_3Cl_{16}$ and $K_7Bi_3Br_{16}$ could be obtained. The procedure is demonstrated in Figure S1. The $K_7Bi_3Cl_{16}$ perovskite single crystals is of white and the $K_7Bi_3Br_{16}$ perovskite single crystals is of pale orange.

Characterizations. $K_7Bi_3X_{16}$(X=Cl, Br) perovskite single crystals were ground to fine power, then characterized by Bruker D8 Advance X-ray diffractometer (XRD) with Cu Kα radiation at 35kV and 20mA. The step and time were set to be 0.01° and 0.1s, respectively. The UV-vis spectra of the single crystals were measured by a double-beam spectrophotometer equipped with integrating sphere (Cary 5000, Agilent technologies). The determination of unit-cell parameters and data collection was performed with XtaLAB PRO CCD area-detector diffractometer, equipped with a

graphite monochromator situated in the incident beam. The single-crystal structure was resolved and refined by SHELXT and OLEX2.[1, 2] Details of X-ray crystallographic parameters are demonstrated in Table S1 and Table S2.

Electronic structure calculations. The density functional theory (DFT) calculations were conducted to explore the electronic structure of the $K_7Bi_3X_{16}$(X=Cl, Br) perovskite structure. The calculation results were obtained by the Real Space Electronic Structure CalcUlator (RESCU), a DFT calculation software package which is based on the Kohn Sham equation:[3]

$$\left[-\frac{1}{2}\nabla^2 + \int d\mathbf{r}' \frac{\rho(\mathbf{r}')}{|\mathbf{r}-\mathbf{r}'|} + V_{ion-e}(\mathbf{r}) + V_{ext}(\mathbf{r}) + V_{xc}(\mathbf{r}) \right] \psi_i(\mathbf{r}) = \varepsilon_i \psi_I \text{®} \quad (1)$$

The method of linear combination of atomic orbitals (LCAO) was chosen to be the calculation framework for all the calculations.[4] The Troullier-Martines norm-conserving pseudopotential was selected to replace the complicated potential derived from the core level electrons and nucleus.[5] The 5×14×3 and 5×5×1 Monkhorst-Pack grid were employed to sample the Brillouin zone of the $K_7Bi_3Br_{16}$ and $K_7Bi_3Cl_{16}$ structure to ensure similar k-point sampling density in three directions of the reciprocal space, respectively.[6] We chose the Perdew-Burke-Ernzerhof (PBE) of generalized gradient approximation (GGA-PBE) exchange-correlation functional to represent the exchange-correlation potential in the Kohn-Sham equation.[7] For the self-consistent calculation, the convergence criteria of $K_7Bi_3X_{16}$ for energy and charge density were set to 1×10^{-6} Hartree and 1×10^{-6} e, respectively, to ensure the calculation accuracy. A real space resolution was set to be 0.5 Bohr. The lattice parameters and atomic coordinates were obtained by crystal resolve and refinement and directly used in the calculation.

Transport properties calculations. In this work, the device models of $K_7Bi_3X_{16}$(X=Cl, Br) were consist of a central region, left and right Au buffer layers and their coherent semi-infinite Au electrodes. The buffer layers comprised 8 atomic layers of Au, and the purpose of which was preventing the mutual interference of the Hartree potential between the central region and the electrodes in the self-consistent calculation. The electrons transported along Z-direction and there was no periodic condition set on the central region on X and Y directions. We employed Nanodcal, an advanced nonequilibrium quantum transport calculation package to study the transport properties of the $K_7Bi_3X_{16}$ (X=Cl, Br) perovskite.[8, 9] The theoretical framework of Nanodcal comprises the combination of the nonequilibrium Green's function (NEGF) theory and the density functional theory (DFT).[10] The linear combination of atomic orbitals (LCAO) framework was selected to conduct the transport property calculations. Again, the Perdew-Burke-Ernzerhof of generalized gradient approximation (GGA-PBE) exchange-correlation functional was employed to represent the exchange-correlation potential. The k-point grid of 1×1×1 and 1×1×100 was set to sample the Brillouin zone of the central region and the electrodes, respectively. The cutoff energy was set to 100 Hartree. The convergence criteria for Hamiltonian and charge density matrix were set to 10^{-4} eV and 10^{-4} e, respectively, for the central region and the corresponding values for electrodes were 10^{-4} eV and 10^{-4} e, respectively, in the self-consistent calculations. The electron spin degenerate condition was considered in the transport property simulations. In this calculation section, the device transmission coefficient Tαβ(ε), which denotes the probability of electrons with energy ε transmitting through the central region from one lead α to another lead β, was calculated by the Green's function:

$$T_{\alpha\beta}(\varepsilon) = tr\left[G^{r}(\varepsilon)\Gamma_{\alpha}(\varepsilon)G^{a}(\varepsilon)\Gamma_{\beta}(\varepsilon)\right] \quad (2)$$

wherein

$$\Gamma_{\alpha}(\varepsilon) \equiv i\left[\sum_{\alpha}^{r}(\varepsilon) - \sum_{\alpha}^{a}(\varepsilon)\right] \tag{3}$$

where $\sum_{\alpha}^{r}(\varepsilon)$ and $\sum_{\alpha}^{a}(\varepsilon)$ denote the retarded and advanced self-energy of lead α, respectively, and $tr\left[G^{r}(\varepsilon)\Gamma_{\alpha}(\varepsilon)G^{a}(\varepsilon)\Gamma_{\beta}(\varepsilon)\right]$ is the trace of $\left[G^{r}(\varepsilon)\Gamma_{\alpha}(\varepsilon)G^{a}(\varepsilon)\Gamma_{\beta}(\varepsilon)\right]$.

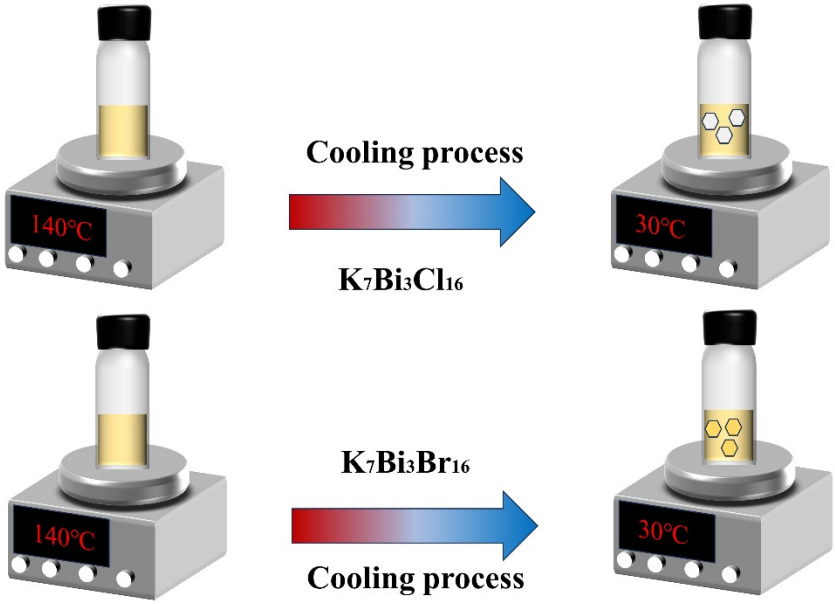

Figure S1. The cooling crystallization method applied for $K_7Bi_3X_{16}$(X=Cl, Br)

Crystal type / Parameter	$K_7Bi_3Br_{16}$
CCDC no.	2303749
Empirical formula	$K_7Bi_3Br_{16}$
Formula weight	2179.20
Crystal system	hexagonal
Space group	$P6_3/m$
Unit-cell dimensions	a= 13.4181(4) Å, b=13.4181(4) Å, c=34.9412(12) Å, α=β=90° γ=120°
Volume	5448.2(4)

Z, density (calculated)	3.985 gcm^{-3}
Absorption coefficient	32.901mm^{-1}
F (000)	5652.0
Crystal size max/mid/min	none
θ range for data collection	3.504-54.284
Index limits	$-16 \leq h \leq 15$, $-9 \leq k \leq 15$, $-43 \leq l \leq 43$
Completeness	97.53
Absorption correction	multi-scan
Refinement method	ShelXL
Data/restraints/parameters	3867 /0/124
Final R indices [I>2σ> 2(I)]	$R_1 = 0.0481$, $wR_2 = 0.0862$
R indices (all data)	$R_1 = 0.0956$, $wR_2 = 0.1019$
goodness-of-fit	0.976
Largest difference map peak/hole	1.39/-2.74$Å^{-3}$

Table S1. Details of X-ray crystallographic parameter of the as-prepared $K_7Bi_3Br_{16}$ perovskite single crystals

Crystal type / Parameter	$K_7Bi_3Cl_{16}$
CCDC no.	2303747
Empirical formula	$K_7Bi_3Cl_{16}$
Formula weight	1467.84
Crystal system	trigonal
Space group	R-3c
Unit-cell dimensions	a=12.8086(3) Å, b=12.8086(3) Å, c= 100.294(3) Å, α=β=90° γ=120°
Volume	14249.8(8)
Z, density (calculated)	3.079 gcm^{-3}
Absorption coefficient	18.897mm^{-1}
F (000)	11772
Crystal size max/mid/min	none
θ range for data collection	1.880-27.159
Index limits	$-16 \leq h \leq 14$, $-8 \leq k \leq 15$, $-121 \leq l \leq 99$
Completeness	95.17
Absorption correction	multi-scan
Refinement method	ShelXL
Data/restraints/parameters	3252/0/121
Final R indices [I>2σ> 2(I)]	$R_1 = 0.0298$, $wR_2 = 0.0757$
R indices (all data)	$R_1 = 0.0436$, $wR_2 = 0.0714$

goodness-of-fit	1.040
Largest difference map peak/hole	1.09/-1.14Å^{-3}

Table S2. Details of X-ray crystallographic parameter of the as-prepared $K_7Bi_3Cl_{16}$ perovskite single crystals

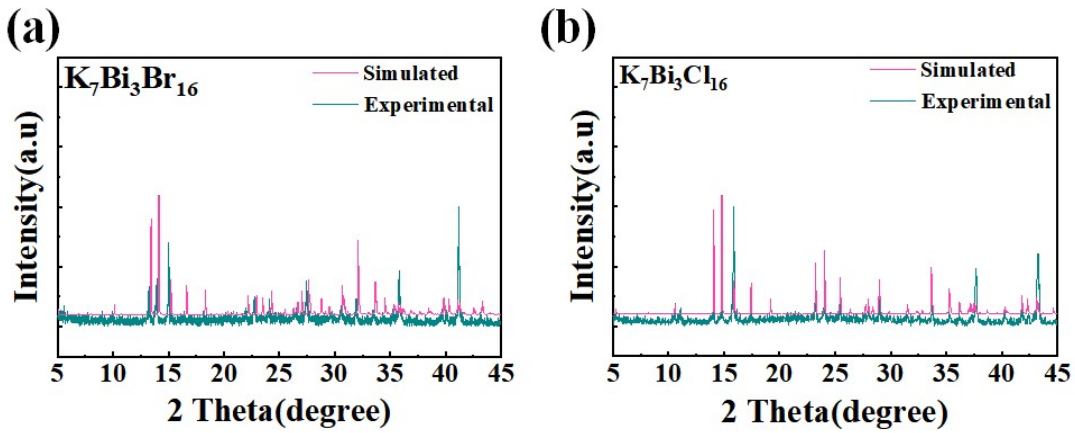

Figure S2. Powder X-ray diffraction patterns comparison between experiment and simulation of (a) $K_7Bi_3Br_{16}$ (b) $K_7Bi_3Cl_{16}$, respectively.

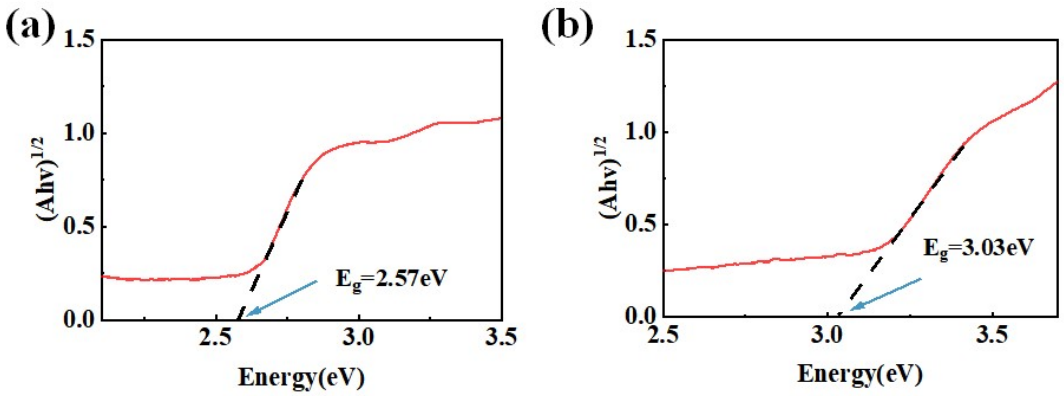

Figure S3. The tauc plot of (a) $K_7Bi_3Br_{16}$ (b) $K_7Bi_3Cl_{16}$ perovskite crystals, which decide their indirect bandgap to be 2.57eV and 3.03eV, respectively.

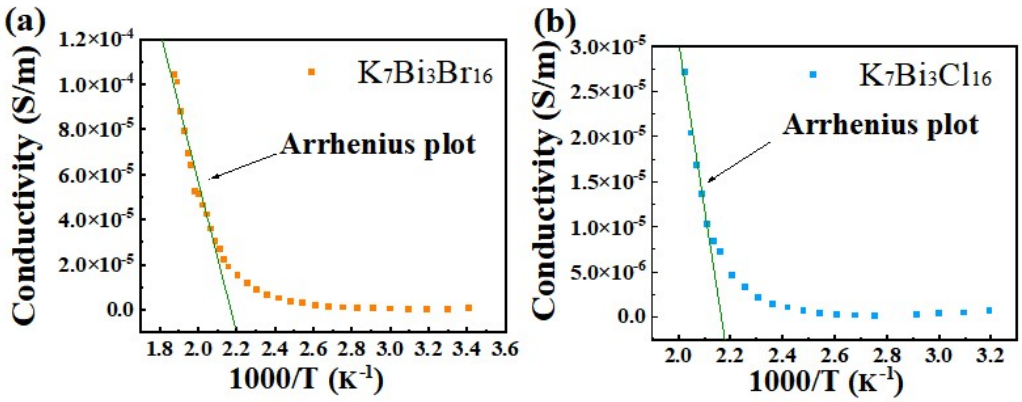

Figure S4. The Arrhenius plot of (a) $K_7Bi_3Br_{16}$ (b) $K_7Bi_3Cl_{16}$ perovskite crystals.

We test the I-V curves of the $K_7Bi_3Br_{16}$ and $K_7Bi_3Cl_{16}$ devices under dark conditions as shown in Figure S5. Figure S5a shows the I-V curve of the $K_7Bi_3Br_{16}$ device in a linear coordinate system, where we see a nonlinear increase in current with increasing voltage, indicating a non-ohmic contact behavior. Figure S5b plots the I-V curve of the $K_7Bi_3Br_{16}$ device in a logarithmic coordinate system, which clarifies the behavior in the low current region. Near zero voltage, the curve exhibits significant asymmetry, a hallmark of Schottky contact[11, 12].

Figure S5c shows an almost linear I-V curve of $K_7Bi_3Cl_{16}$ device in a linear coordinate system, suggesting a proportional relationship between current and voltage, consistent with Ohm's law, indicative of ohmic contact behavior[12]. Figure S5d, as in the logarithmic coordinates also shows good symmetry, a sign of ohmic contact between the $K_7Bi_3Cl_{16}$ and the electrodes.

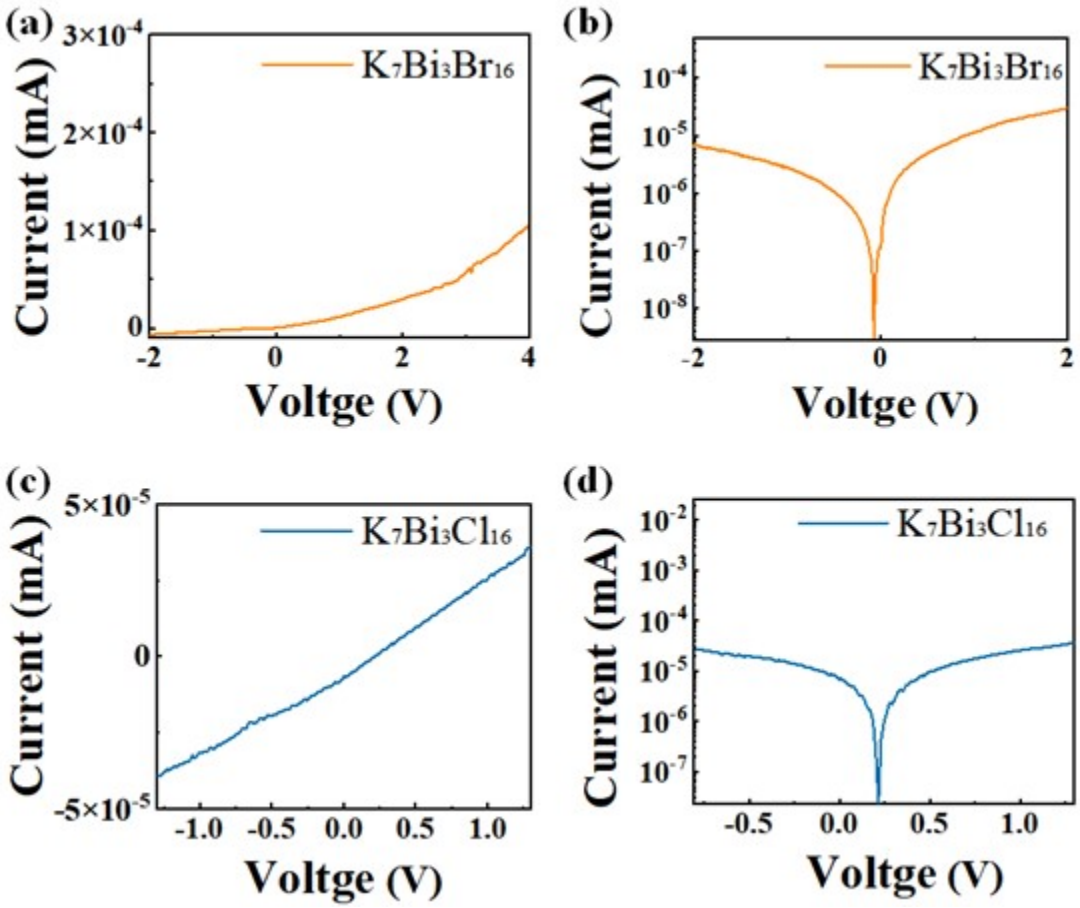

Figure S5. The rectangular I-V curves of of (a) $K_7Bi_3Br_{16}$ (c) $K_7Bi_3Cl_{16}$ perovskite crystal devices and the logarithmic I-V curves of of (b) $K_7Bi_3Br_{16}$ (d) $K_7Bi_3Cl_{16}$ perovskite crystal devices. $K_7Bi_3Br_{16}$ forms Schottky contact with the electrodes and the $K_7Bi_3Cl_{16}$ forms Ohmic contact with the electrodes.

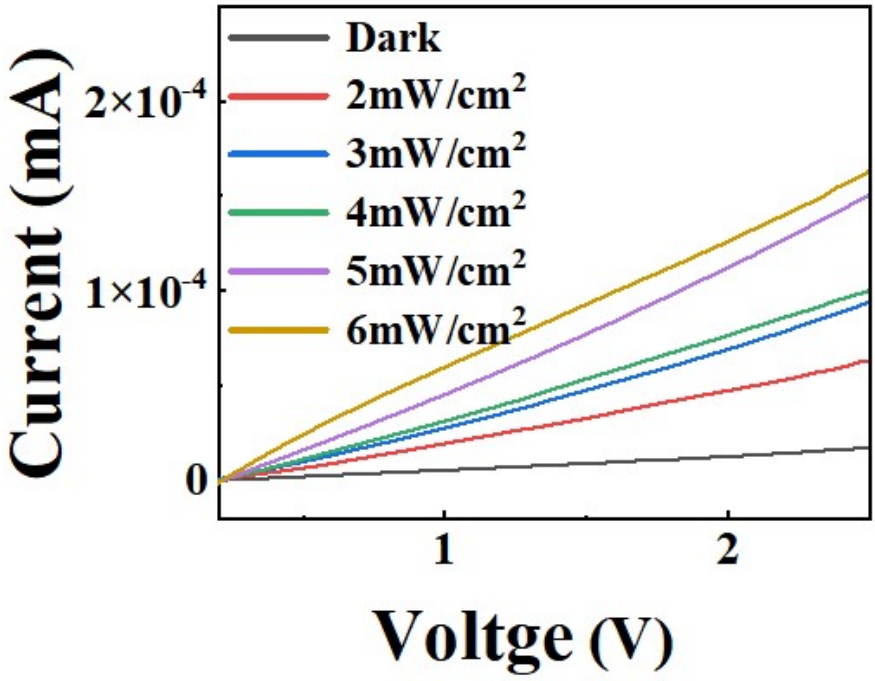

Figure S6. Response light current of $K_7Bi_3Br_{16}$ photodetector under 395 nm radiation of various intensity.

References.

1. G. Sheldrick, *Program for crystal structure refinement*, 1997.
2. G. Sheldrick, 2003.
3. W. Kohn and L. J. Sham, *Physical review*, 1965, **140**, A1133.
4. P. Hohenberg and W. Kohn, *Physical review*, 1964, **136**, B864.
5. N. Troullier and J. L. Martins, *Physical review B*, 1991, **43**, 1993.
6. H. J. Monkhorst and J. D. Pack, *Physical review B*, 1976, **13**, 5188.
7. J. P. Perdew, K. Burke and M. Ernzerhof, *Physical review letters*, 1996, **77**, 3865.
8. D. Waldron, P. Haney, B. Larade, A. MacDonald and H. Guo, *Physical review letters*, 2006, **96**, 166804.
9. D. Waldron, L. Liu and H. Guo, *Nanotechnology*, 2007, **18**, 424026.
10. J. Taylor, H. Guo and J. Wang, *Physical Review B*, 2001, **63**, 245407.
11. R. Long, B. Li and Q. Mi, *AIP Advances*, 2020, **10**.
12. C.-H. Lin, T.-Y. Li, B. Cheng, C. Liu, C.-W. Yang, J.-J. Ke, T.-C. Wei, L.-J. Li, A. Fratalocchi and J.-H. He, *Nano Energy*, 2018, **53**, 817-827.